Achieving High Dielectric Constant and Low Loss Property in a Dipolar Glass Polymer Containing Strongly Dipolar and Small-Sized Sulfone Groups

Junji Wei,[†,‡] Zhongbo Zhang,[‡] Jung-Kai Tseng,[‡] Imre Treufeld,[‡] Xiaobo Liu,[†] Morton H. Litt,*[,‡] and Lei Zhu*[,‡]

[†]Institute of Microelectronics and Solid State Electronics, University of Electronic Science and Technology of China, Chengdu, Sichuan, P. R. China

[‡]Department of Macromolecular Science and Engineering, Case Western Reserve University, Cleveland, Ohio 44106-7202, United States

ⓈSupporting Information

ABSTRACT: In this report, a dipolar glass polymer, poly(2-(methylsulfonyl)ethyl methacrylate) (PMSEMA), was synthesized by free radical polymerization of the corresponding methacrylate monomer. Due to the large dipole moment (4.25 D) and small size of the side-chain sulfone groups, PMSEMA exhibited a strong γ transition at a temperature as low as −110 °C at 1 Hz, about 220 °C below its glass transition temperature around 109 °C. Because of this strong γ dipole relaxation, the glassy PMSEMA sample exhibited a high dielectric constant of 11.4 and a low dissipation factor (tan δ)

of 0.02 at 25 °C and 1 Hz. From an electric displacement-electric field (D-E) loop study, PMSEMA demonstrated a high discharge energy density of 4.54 J/cm³ at 283 MV/m, nearly 3 times that of an analogue polymer, poly(methyl methacrylate) (PMMA). However, the hysteresis loss was only 1/3−1/2 of that for PMMA. This study suggests that dipolar glass polymers with large dipole moments and small-sized dipolar side groups are promising candidates for high energy density and low loss dielectric applications.

KEYWORDS: dipolar glass polymer, orientational polarization, sub-T_g transition, dielectric constant, broadband dielectric spectroscopy, electric energy storge
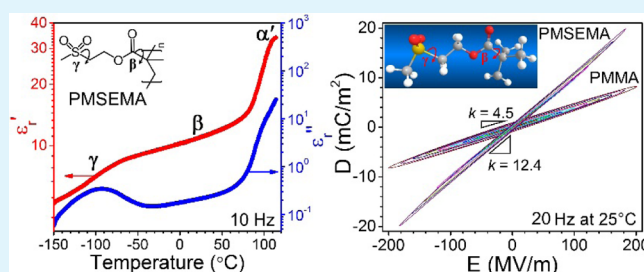
1. INTRODUCTION

Polymer dielectrics are important materials for advanced electrical and power applications.[1,2] With the development in power electronics such as electric motors for electrical and hybrid electric vehicles, next-generation polymer dielectrics with high energy density, high temperature capability, as well as low dielectric loss are highly desirable. For linear dielectric polymers, the energy density can be calculated as $U_e = 0.5k\varepsilon_0 E^2$, where k is the relative dielectric constant, ε_0 the vacuum permittivity, and E the applied electric field.[3] To increase electric energy storage, increasing breakdown strength seems to be more attractive than increasing dielectric constant, because U_e scales as the second power of the electric field. However, it is fairly difficult to substantially increase the breakdown strength for polymer films because of two reasons. First, the highest electrical breakdown strength is observed for inorganic single crystals, such as diamond, around 2 GV/m.[4] Current state-of-the-art polymer dielectric material, such as biaxially oriented polypropylene (BOPP), has already reached a breakdown strength of 730 MV/m.[5] It is difficult to further enhance electrical breakdown strength for polymers. Second, the much lower engineering breakdown strength than the intrinsic

breakdown strength[6] (around 10 GV/m) at a band gap of 8 eV (e.g., for polyethylene[7]) must originate from impurities and manufacturing defects in polymer films. Therefore, it is more practical to increase the dielectric constant, rather than electrical breakdown strength. This requires us to understand the fundamental polarization mechanisms in organic polymers.

As we know, there are five types of polarization for polymers, namely, electronic, atomic (or vibrational), orientational (or dipolar), ionic, and interfacial polarization.[2,8,9] Electronic and atomic polarizations occur at very high frequencies, namely, in the infrared and optical ranges.[8,9] It is the most desired to utilize both polarizations to increase dielectric constants of polymers because they show no losses in the power and radio frequencies. However, a recent computational study showed that only limited increases in dielectric constant could be achieved without significantly decreasing the band gap of polymers.[10] For example, the dielectric constant for carbon-based polymers was limited to 4 and 7 for the band gap being 5

and 3 eV, respectively. On the other hand, interfacial[8,11] and ionic[12] polarizations are not desirable for film capacitor applications because they involve slow discharge processes and their dielectric losses are relatively high. This leaves only the dipolar polarization to enhance the dielectric constant of polymers while having low dielectric losses.

To utilize dipolar polarization, we should be aware of several strategies together with certain caution. First, normal ferroelectric polymers should be avoided for film capacitor applications because of their high hysteresis losses (>80−90% loss).[2] Typical examples include odd-numbered nylons, poly-(vinylidene fluoride) (PVDF) and its random copolymers with trifluoroethylene (TrFE), tetrafluoroethylene (TFE), chlorotrifluoroethylene (CTFE), and hexafluoropropylene (HFP).[13] Instead, relaxor ferroelectric polymers showing narrow double or single hysteresis loops are promising for high energy density and low loss polymer dielectrics.[1,2,14] Because of the formation of nanosized ferroelectric domains (or nanodomains) in isomorphic crystals, high dielectric constants in the range of 30−70 can be achieved with fairly low hysteresis loss. Typical examples of relaxor ferroelectric polymers are electron beam-irradiated P(VDF-TrFE)[15,16] and P(VDF-TrFE)-based random terpolymers [e.g., P(VDF-TrFE-CFE) (CFE is 1,1-chlorofluoroethylene) and P(VDF-TrFE-CTFE)].[17−20] Nonetheless, these relaxor ferroelectric polymers still suffer from low Curie temperatures (around room temperature) and low melting points (ca. 125 °C), and thus exhibit relatively high conduction losses above the Curie temperature.[14]

A better candidate for high energy density, high temperature, and low loss dielectrics is dipolar glass polymers. From our recent perspective article,[1] a dipolar glass polymer shall have a high glass transition temperature (T_g) and a significant dipolar polarization in sub-T_g transitions. The high T_g can prevent losses from electronic and ionic conductions, and the sub-T_g transition due to dipole rotation will enhance the dielectric constant. The temperature difference between the T_g and the sub-T_g transitions needs to be large enough to ensure a broad window for practical applications. One strategy is to dope a glassy polymer with dipolar molecules via either simple blending or molecular (covalent) labeling. Note that these large dipole moment molecules often have high nonlinear optical responses.[21,22] For simple blending, the content and molecular size of the dopant molecules are important. First, the content of the dopant molecules shall be low enough to avoid macrophase separation. Even at a few percent of the dopant molecules, the T_g of the polymer matrix will significantly decrease due to the plasticization effect.[23] Second, when the molecular size is larger than 0.6 nm, the dopant molecules will have difficulty to rotate in the glassy polymer matrix.[24] As a result, the sub-T_g transition due to the rotation of dopant molecules often overlaps with the glass transition of the polymer matrix. For molecular labeling, the dipolar monomers are copolymerized into the backbone of a glassy polymer.[25] Again, because of the large size and small fraction of the labeling comonomer, the sub-T_g transition from rotation of dipolar side chains is located fairly close to the glass transition. In both blending and labeling of dipolar molecules, the increase in dielectric constant (or dielectric relaxation strength[9]) for the nonpolar polymer matrix has been limited to below 1 due to a low content of the dopant molecules.

Instead of using large dipolar molecules, which are difficult to rotate in the glassy polymer matrix, it is highly desirable to attach small dipolar groups to polymer chains in order to

achieve easy dipole rotation. Two ways have been explored, namely, main-chain and side-chain dipoles. When dipolar groups, such as −F and −CN, are directly attached to the main-chain polymers, limited enhancement in dielectric constant and relatively high dielectric loss are observed due to the difficulty in rotating main-chain dipoles.[26−28] When dipolar groups are attached in the side chains, easier rotation of the side groups can substantially increase the dielectric constant while keeping the dielectric loss relatively low. For example, when −CH$_2$CN groups were attached as the side chains in a bisphenol A polycarbonate (i.e., CN-PC), the dielectric constant increased to 4.0 for CN-PC as compared to that of 2.9 for neat PC at 1 kHz.[29] The dielectric loss was reasonably low, namely, tan $\delta \sim$ 0.005 at 130 °C and 1 kHz. Furthermore, cyanoethylated poly(2,3-dihydroxylpropyl methacrylate) (CN$_2$-PDPMA) exhibited a relatively high dielectric constant (ca. 8) between the β (rotation of −CH$_2$CH$_2$CN dipoles at −60 °C) and the α (T_g at 25 °C) transitions at 500 Hz.[30] However, the window between the β and α transitions was only 85 °C, which is not broad enough for practical applications such as film capacitors.

To enable practical film capacitor application, it is desirable to further enhance the dielectric constant (above 10) and broaden the window between the sub-T_g and T_g transitions (e.g., above 200 °C). In this work, we report synthesis and dielectric properties of a model dipolar glass polymer containing polar sulfone groups, i.e., poly(2-(methylsulfonyl)-ethyl methacrylate) (PMSEMA). The dipole moment of the sulfone group is as large as 4.25 Debye (D), even higher than that of the CN dipole (3.9 D).[28−30] Meanwhile, the required space (or the size) of the sulfone group (32.3 Å^3 and 2.5 Å in length) is smaller than that of the −CH$_2$CN group (34.7 Å^3 and 3.5 Å in length), making its rotation in the glassy polymer even easier. Therefore, we expect that the dielectric properties of PMSEMA are superior to those of −CH$_2$CN containing polymers. Indeed, a high dielectric constant of 11−12 and a reasonably low dissipation factor (tan $\delta \sim$ 0.02) are obtained for PMSEMA at 25 °C and 1 Hz. The window between the γ (ca. −110 °C) and α (ca. 109 °C) transitions is as large as ca. 220 °C. Therefore, side-chain sulfone-containing polymers are promising for high dielectric constant and low loss dielectric applications.

2. EXPERIMENTAL SECTION

2.1. Materials. 2-(Methylsulfonyl)ethanol (98%), methacryloyl chloride, triethylamine (Et$_3$N), and azobis(isobutyronitrile) (AIBN) were purchased from Sigma-Aldrich. All solvents were purchased from Fisher Scientific.

2.2. Synthesis of 2-(Methylsulfonyl)ethanol (MSEMA). MSEMA was prepared by reacting 2-(methylsulfonyl)ethanol with methacryloyl chloride in the presence of Et$_3$N (see Scheme 1). A 100 mL three-neck flask was charged with 4.52 g (0.036 mol) of 2-(methylsulfonyl)ethanol, 40 mL of dichloromethane (DCM), and 5.12 g (0.0506 mol) of Et$_3$N. The mixture was stirred with dry N$_2$ purging in an ice bath for 30 min. Then, 4.6 g (0.044 mol) of methacryloyl

Scheme 1. Synthesis of the Dipolar Glass Polymer, PMSEMA
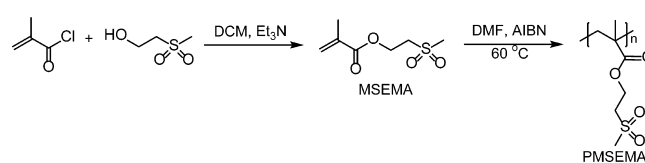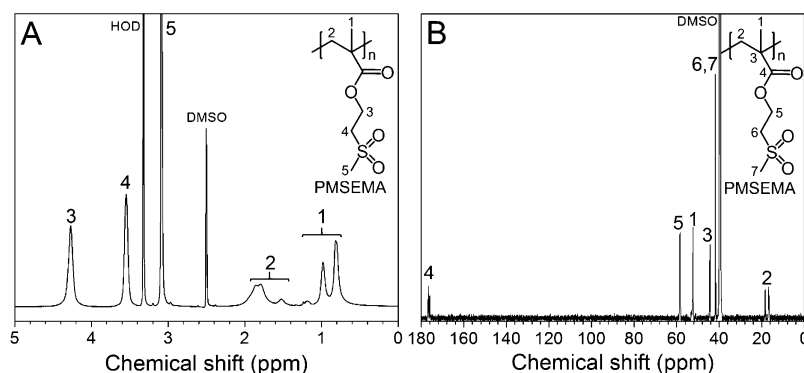
Figure 1. (A) ^{1}H and (B) ^{13}C NMR spectra of PMSEMA. The solvent is DMSO-d_6. Peak assignments are shown, together with indication of solvent and water peaks.

chloride was added to the mixture dropwise. The reaction was slowly warmed up to room temperature over 24 h. After the reaction, triethylamine hydrochloride was removed by filtration. The remaining solvent was removed using reduced pressure distillation. The crude product was redissolved in DCM and precipitated into diethyl ether, and the dissolution−precipitation process was repeated for three times. Finally, the as-prepared monomer was dried in a vacuum oven at room temperature for 2 days. The yield was about 60%. ^{1}H nuclear magnetic resonance (NMR) (CDCl$_3$, δ): 1.96 (s, 3H, −CCH_3), 2.99 (s, 3H, −SO$_2$CH_3), 3.38 (t, 2H, −SO$_2$CH_2CH$_2$O−), 4.62 (t, 2H, −SO$_2$CH$_2$CH_2O−), 5.65 (s, 1H, −C(CH$_3$)=CH_2), 6.14 (s, 1H, −C(CH$_3$)C=CH_2). ^{13}C NMR (CDCl$_3$, δ): 16.7 (−CCH$_3$), 40.7 (−SO$_2$$CH_3$), 52.4 (−SO$_2$$CH_2CH_2$O−), 56.7 (−SO$_2CH_2$$CH_2$O−), 125.3 (−C(CH$_3$)=$CH_2$), 134.0 (−$C$(CH$_3$)=CH$_2$), 165.0 (−O$C$OC-(CH$_3$)−). The purified monomer showed a melting peak at 49 °C.

2.3. Synthesis of PMSEMA. PMSEMA was synthesized by free radical polymerization from MSEMA monomer using AIBN as initiator. In detail, 15.34 mg (0.093 mmol) of AIBN was dissolved in 10 mL of N,N-dimethylformamide (DMF). A 10 mL ampule was charged with 0.2 g (1 mmol) of MSEMA, 1 mL of AIBN DMF solution, and a small magnetic stirrer. Then, the ampule was frozen in liquid nitrogen before applying a high vacuum (20 mTorr). After three freeze−pump−thaw cycles, the ampule was sealed under vacuum using a torch. The free radical polymerization was carried out at 60 °C for 24 h. The solution was precipitated in ethanol. The as-prepared PMSEMA was redissolved in DMF and precipitated into methanol, and the dissolution−precipitation process was repeated for three times. The precipitated polymer was further soaked in deionized water for 3 days (the water was changed twice everyday) in order to completely remove residue DMF and impurity ions. Finally, the purified polymer was dried in a vacuum oven at 50 °C for 3 days before storing in a desiccator at ambient temperature.

2.4. Characterizations. ^{1}H and ^{13}C NMR spectra were recorded using Varian Mercury 300 and 600 MHz NMR spectrometers, respectively. The solvent was CDCl$_3$ for MSEMA and DMSO-d_6 for PMSEMA. Thermal behavior of MSEMA and PMSEMA was studied using a TA Instruments Q100 differential scanning calorimeter (DSC) and Q500 thermogravimetric analysis (TGA). The heating rates for DSC and TGA were 10 and 20 °C/min, respectively. The molecular weight of PMSEMA was determined by size-exclusion chromatography (SEC) using a Water 515 HPLC pump and Waters 717 Auto Injector, equipped with a Waters 2414 differential refractive index detector. N,N-Dimethylacetamide (DMAc) was used as the solvent at a flow rate of 1.0 mL/min. Two Jordi gel divinylbenzene (DVB) mixed bed columns (25 cm × 10 cm, 5 μm pore size) were used at 80 °C. Polystyrene (PS) was used as the standard for conventional calibration. Fourier transform infrared (FTIR) spectra were obtained using a Bomem Michelson MB100 FTIR spectrometer, which was equipped with a deuterated triglycine sulfate (DTGS) detector and a dry air purge unit. A total of 64 scans were recorded at a resolution of 4 cm^{-1}. Transmission FTIR spectra were obtained using pellets

prepared by grinding solid samples with potassium bromide (KBr) powder.

The density measurement for PMSEMA was carried out by the suspension method. First, the PMSEMA was hot-pressed into a bubble-free film. Then, it was placed into a glass vial with mixed diethyl ether (density of 0.713 g/cm^3) and chloroform (density of 1.48 g/cm^3). After sonication to remove surface bubbles, the film was suspended in the mixed solvent by adjusting the ratio of diethyl ether to chloroform. The suspension should be stable for at least 1 h. The density of the mixed solvent was taken as the density of the PMSEMA film.
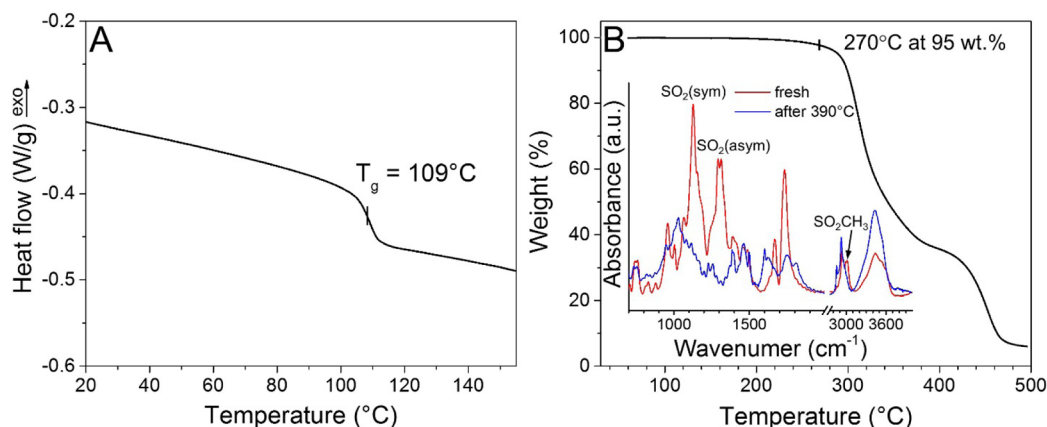
Broadband dielectric spectroscopy (BDS) measurements were performed on a Novocontrol Concept 80 broadband dielectric spectrometer with temperature control. The applied voltage was 1 Vrms (rms means root-mean-square) with the frequency ranging from 0.01 Hz to 10 MHz and the temperature from −150 to 120 °C. Silver electrodes (100 nm thick) were evaporated by electron beam (EvoVac Deposition System, Angstrom Engineering Inc.) onto Kapton films, which was often used as a strong flexible backing to survive hot-press at high temperatures (up to 250 °C). The electrode area was ca. 0.786 cm^2. The dried PMSEMA powder was sandwiched between two Kapton films with silver electrodes and then hot-pressed at 150 °C into 174 μm thick bubble-free films for BDS measurements.

The electric displacement-electric field (D-E) hysteresis loop measurements were carried out using a Premiere II ferroelectric tester (Radiant Technologies, Inc.) equipped with a Trek 10/10B-HS high voltage amplifier (0−10 kV AC). The applied voltage had a bipolar sinusoidal waveform ranging from 10 to 2000 Hz. The sample was immersed in a silicone oil bath during tests, and the temperature was varied from 25 to 75 °C. The temperature was controlled using an IKA RCT temperature controller. The hot-pressed PMSEMA (about 50 μm thick) sandwiched between two silver electrode-coated Kapton films were prepared similarly to those for the BDS measurements, except that the electrode area was ca. 0.0515 cm^2. For the solution-cast film, the PMSEMA solution in redistilled DMF (20 mg/mL) was drop-cast onto a Kapton film coated with Ag electrode. The sample was dried at ambient temperature for 2 days and then at 110 °C in a vacuum oven for 4 days. The final film thickness was around 26.1 μm.
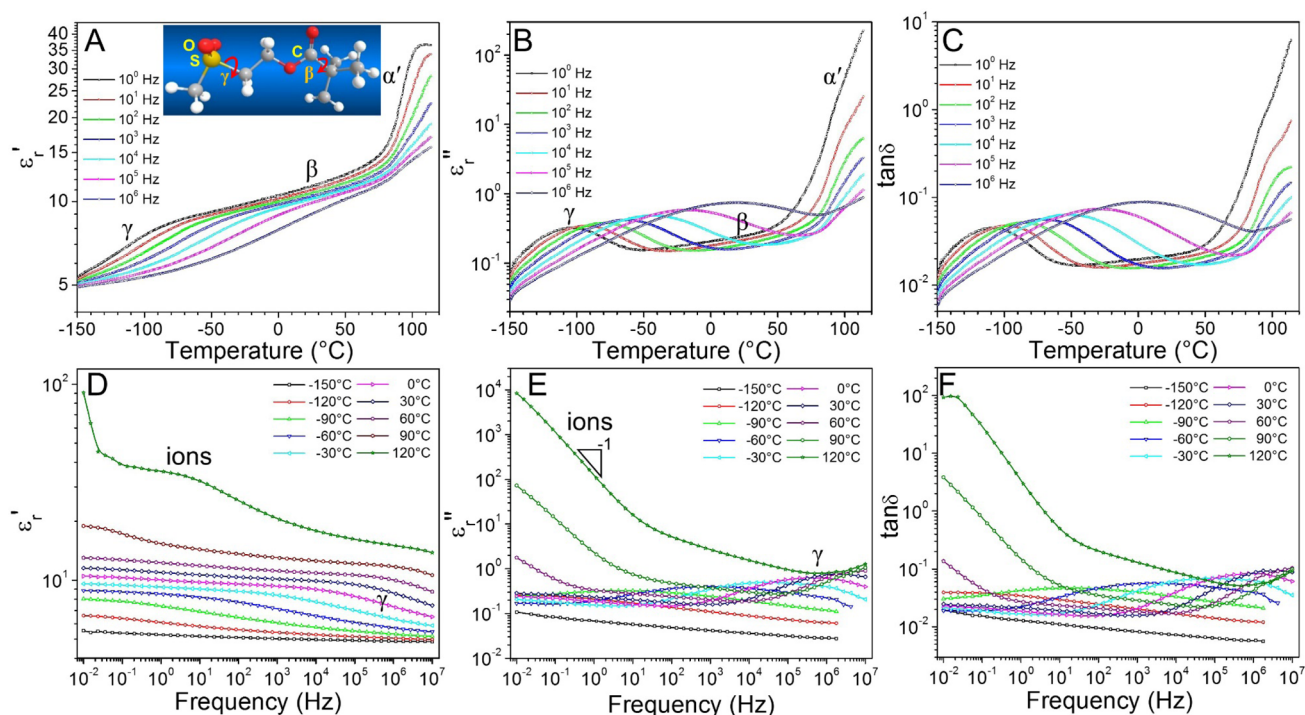
Note that Kapton films were outside of the Ag electrodes, which were directly connected to an external cathode and anode. Therefore, the Kapton film would not affect the BDS and D-E loop measurements of the sample. This sample preparation method was verified for known polymer samples, such as PS and poly(methyl methacrylate) (PMMA); see Figure S1 in the Supporting Information. The measured dielectric constants for the hot-pressed PS and PMMA samples were 3.0 (by BDS) and 3.3−4.0 (by D-E loop), respectively, similar to the literature values for PS (2.6−3.0) and PMMA (2.8−4).[31]

3. RESULTS AND DISCUSSION

Scheme 1 shows the synthesis of PMSEMA from MSEMA using conventional free radical polymerization initiated by

Figure 2. (A) DSC and (B) TGA curves for PMSEMA. The DSC and TGA heating rates are 10 and 20 °C/min, respectively. The inset in (B) shows FTIR spectra for PMSEMA before and after being heated under a dry N_2 atmosphere in TGA.
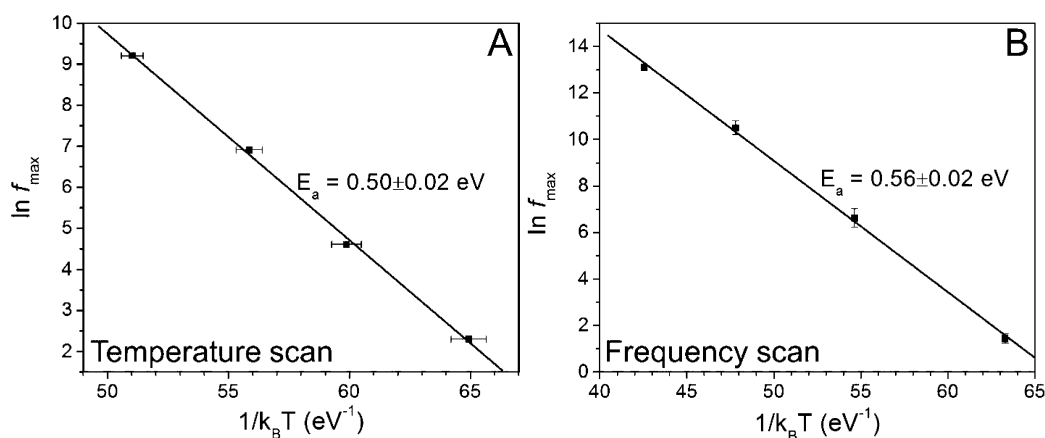

Figure 3. (A) Real (ε_r') and (B) imaginary (ε_r'') parts of relative permittivity and (C) dissipation factor (tan δ) as a function of temperature at different frequencies for PMSEMA. (D) ε_r', (E) ε_r'', and (F) tan δ as a function of frequency at different temperatures for PMSEMA.

AIBN in DMF at 60 °C. The MSEMA monomer was synthesized by reacting the 2-(methylsulfonyl)ethanol with methacryloyl chloride in DCM in the presence of Et$_3$N. The structure of the purified MSEMA was confirmed by ^{1}H and ^{13}C NMR spectroscopy and had a melting point of 49 °C. Polymer molecular weight was measured by SEC using DMAc as the solvent and PS standards for conventional calibration. A symmetric unimodal peak was observed. The number-average molecular weight was 58 000 g/mol, and the molecular weight distribution was 3.1. Although this molecular weight appears relatively low for good mechanical properties, the dielectric constant and polarization of a polymer are not much influenced by its molecular weight. In the future, we will optimize our synthesis for higher molecular weight samples and study their mechanical and rheological properties. Note that high molecular weight and optimal rheological properties are required for biaxial stretching of amorphous polymers (e.g.,

PS) in order to obtain thin film thickness (ca. 10 μm). The PMSEMA was soluble in polar solvents such as DMF and dimethyl sulfoxide (DMSO), but not in acetone, diethyl ether, tetrahydrofuran (THF), chloroform, or toluene. Figure 1A,B shows ^{1}H and ^{13}C NMR spectra of purified PMSEMA. By comparing the ^{1}H and ^{13}C NMR spectra of PMMA,[32] all protons and carbons in the repeat unit can be successfully assigned. Main-chain protons and carbons showed multiple peaks due to random tacticity.

Neat PMSEMA was an amorphous polymer and showed a T_g around 109 °C at a heating rate of 10 °C/min (see Figure 2A). Due to strong dipolar interactions among sulfone side groups, this T_g was much higher than that for an analogue polymer, poly(n-butyl methacrylate) (PnBMA, T_g = 20 °C), but similar to that for PMMA (T_g = 105 °C). The TGA result in Figure 2B showed that 5 wt % degradation started around 270 °C, above which two-step degradation processes were seen. The first step

Figure 4. Arrhenius plots of ln f_{max} versus $1/k_B T$ for the (A) temperature- and (B) frequency-scan BDS results in Figure 3.

degradation lost ca. 65 wt % weight around 310 °C, and the second step lost ca. 30 wt % weight around 450 °C with 5 wt % charcoal formation under a nitrogen atmosphere. From calculation, the $-OCH_2CH_2SO_2CH_3$ side chain occupies about 65 wt % of a repeat unit. We speculate that the first step degradation was thermal cleavage of the $-OCH_2CH_2-SO_2CH_3$ side groups. This was proved by FTIR results for PMSEMA before and after being heated to 390 °C in a dry nitrogen atmosphere in TGA (the sample was cooled down to room temperature before exposure to the air). From the inset of Figure 2B, the IR absorption bands at 1126 (SO_2, symmetric stretching), 1313 (SO_2, asymmetric stretching), and 3015 cm^{-1} (C−H stretching in SO_2CH_3) disappeared after heating PMSEMA to 390 °C. This result clearly indicated that the first step degradation is the cleavage of the (2-methylsulfonyl)-ethyl side group. We speculate that this side-chain cleavage is closely related to the electron withdrawing property of the methylsulfonyl group.
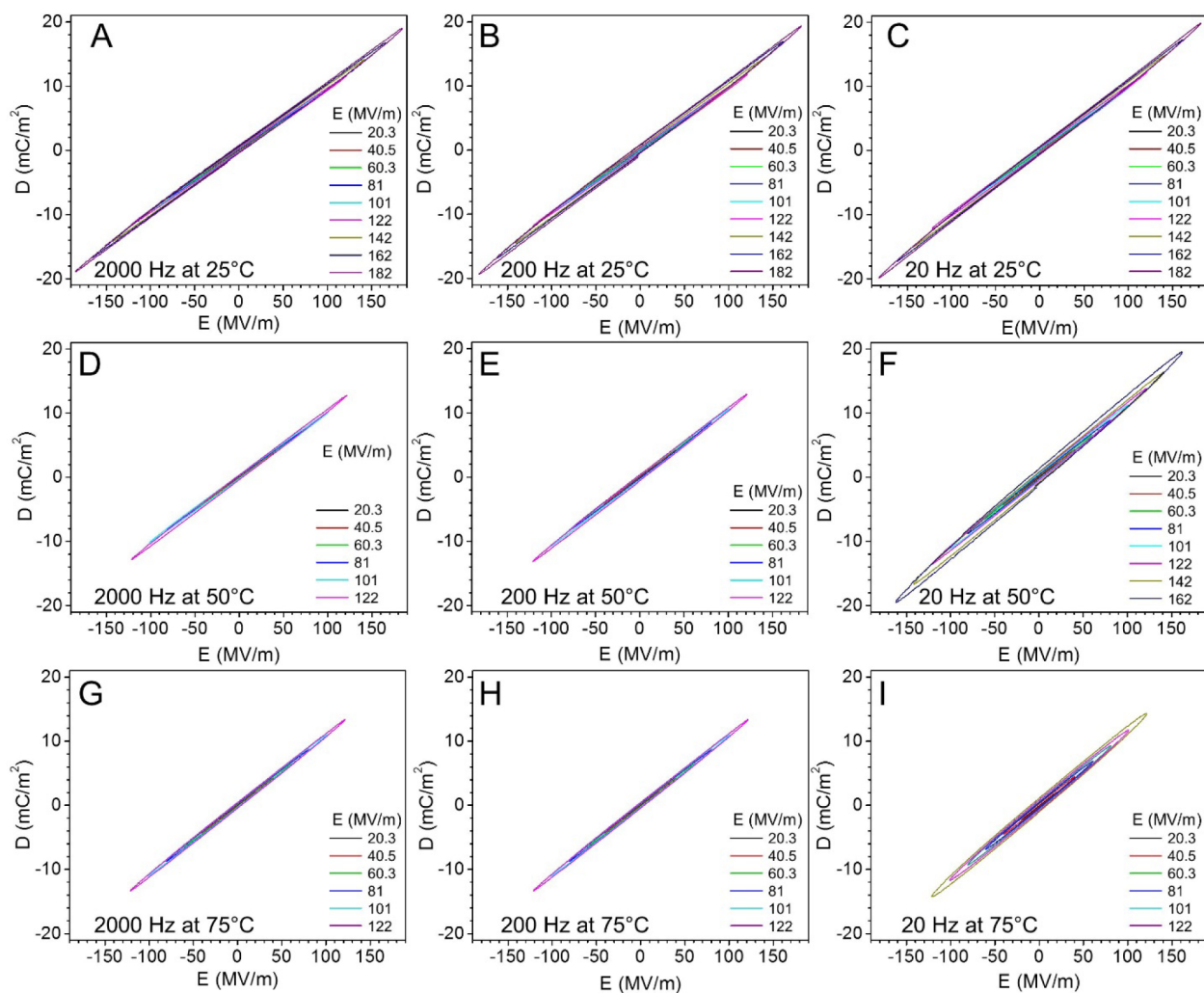
The dipole moment of the sulfonyl group is 4.25 D. The dipole moments for the ester group is 1.75 D. If we assume the side chain atoms are in an all trans conformation, the total dipole moment of the MSEMA repeat unit would be about 6.0 D, if the ester and sulfone groups can align parallel (see Scheme 1). Taking into account the density of PMSEMA of ca. 1.39 g/cm^3, the dipole moment density was calculated to be 2.6×10^{28} D/m^3. This is higher than that ($\sim 1.0 \times 10^{28}$ D/m^3) of CN-PC[29] and only slightly lower than that ($\sim 3.5 \times 10^{28}$ D/m^3) of CN$_2$-PDPMA.[30] Therefore, we would expect a high dielectric constant for PMSEMA if the sulfonyl groups could easily rotate in response to the external electric field.

To test this hypothesis, low-field BDS was performed. Figure 3 shows both temperature- and frequency-scan BDS results for PMSEMA. From Figure 3A,B, two obvious transitions could be identified between −150 and 120 °C. First, a high temperature transition was observed around 94 °C, above which the ε_r' reached a plateau value of 36.6 at 1 Hz (Figure 3A). Note that this temperature was about 15 °C below the T_g value detected by DSC. We speculated that BDS should be sensitive to dipole motions, which might take place somewhat below the cooperative segmental motions during the glass transition. Therefore, we tentatively assigned this high temperature transition as an α' transition. Second, a γ transition was observed around −110 °C at 1 Hz, which could be attributed to the switching of side-chain sulfone dipoles under the alternating electric field. Upon increasing frequency, both γ and α'

transitions shifted to higher temperatures. Between the γ and α' transitions, ε_r' gradually increased from 9.2 at −50 °C to 12.5 at 50 °C at 1 Hz. It is reported that the β transition for polymethacrylates is between 10 and 60 °C, regardless of the length of the alkyl side chains (e.g., methyl, ethyl, propyl, and butyl), which is attributed to the rotation of ester groups in the side chains.[33,34] Therefore, we consider that the gradual increase in ε_r' between 0 and 60 °C could be assigned as a weak β transition due to the rotation of the ester groups.[35] If this is the case, the γ transition in PMSEMA shall be attributed to the rotation of the sulfone groups. Note that similar γ transitions are also observed for polymethacrylates with long alkyl side chains such as isobutyl and n-butyl groups.[33,36] However, these γ transitions are fairly weak due to the weak polarity of the long alkyl side chains. Ideally, direct and accurate assignment of the β and γ transitions can only be achieved by solid-state multidimensional ^{13}C NMR, which is similar to the work performed for PMMA in ref 34. In the future, we will pursue this effort through potential collaborations.

From this BDS result, we can define the glassy PMSEMA between −80 and 90 °C as a dipolar glass polymer, rather than a paraelectric polymer. As we discussed in ref 1, both dipolar glass and paraelectric polymers show a more or less linear D-E hysteresis loop before dipole saturation. However, the dipole–dipole interaction is weaker in a dipolar glass polymer than in a paraelectric polymer. Consequently, a dipolar glass polymer will exhibit a lower dielectric constant (or dipolar polarization) than a paraelectric polymer. This is exactly seen for PMSEMA in Figure 3A. Below the T_g around 94 °C, the dielectric constant of glassy PMSEMA is about 11.4 at room temperature and 1 Hz. Above the T_g, the dielectric constant of molten PMSEMA is as high as 36.6 at 1 Hz. Obviously, the translational motion in addition to the rotational motion of the molecular dipoles in the polymer melt enhances the dipole–dipole interaction. Therefore, we conclude that the glassy PMSEMA between −80 and 90 °C is a dipolar glass polymer, whereas molten PMSEMA above 100 °C is a paraelectric polymer.

Figure 3D,E shows frequency-scan results at different temperatures. Between −120 and 60 °C, ε_r' gradually decreased with increasing frequency; this could be attributed to the relaxation of sulfone dipoles. Corresponding dipole dispersion peaks in ε_r'' were observed at different temperatures, e.g., 6.5 Hz at −90 °C, 1.15 kHz at −60 °C, 36.5 kHz at −30 °C, 487 kHz at 0 °C, and 1.78 MHz at 30 °C. Obviously, the peak frequency increased with increasing temperature. Above 90 °C,

Figure 5. Bipolar D-E loops for a hot-pressed PMSEMA film (42.5 μm) at (A–C) 25 °C, (D–F) 50 °C, and (G–I) 75 °C at different frequencies: (A, D, G) 2000 Hz, (B, E, H) 200 Hz, and (C, F, I) 20 Hz.

contribution from impurity ions started to be seen in Figure 3D,E, because both ε_r' and ε_r'' increased with decreasing frequency. In other words, ionic polarization could be ignored when the temperature was below 75 °C and the dielectric constant increase could be attributed to the dipolar polarization. ε_r'' versus frequency had a slope of −1 below 10 Hz in the double logarithmic plot. For polar polymers, trace amounts of impurity ions are difficult to avoid, and even sub-ppm levels of impurity ions could cause a significant loss.[37−39] Because of the dipole motions, ε_r' reaches about 11.4 at 25 °C and 1 Hz, together with a reasonably low dielectric loss, i.e., tan δ = 0.02. The window between γ (ca. −110 °C) and α' (94 °C) transitions is as large as ca. 204 °C. In addition, the γ dipole relaxation takes place at a high frequency of ca. 1 MHz around room temperature. All of these dielectric properties suggest that PMSEMA shall be a good candidate for room temperature, high dielectric constant, and low loss dielectric film capacitor applications.
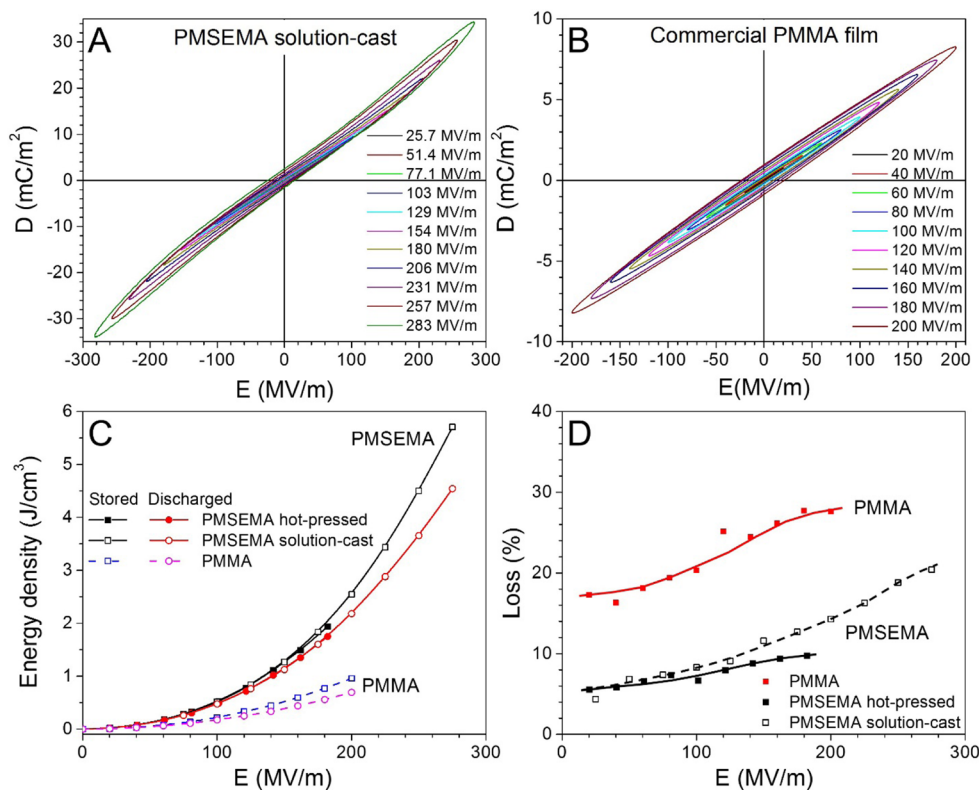
The activation energy for the γ transition could be estimated by the Arrhenius equation from both temperature- and frequency-scan BDS results in Figure 3,[33] and results are shown in Figure 4A,B, respectively. The activation energy was determined to be 0.50 ± 0.02 and 0.56 ± 0.02 eV for temperature- and frequency-scan BDS results. These activation

energy values for the γ transition were considerably lower than those reported for the β transitions in polymethacrylates with methyl, ethyl, and n-butyl groups, i.e., ca. 0.83 eV.[33] Assuming the ester group had the same activation energy as those in polymethacrylates, our result indicated that the rotation of the sulfone groups was easier than the ester groups in the side chains of PMSEMA. It is considered that the size of sulfone groups is small enough so that they can more easily rotate in the free volume of the glassy polymer matrix.

Currently, there has been no available theoretical prediction for orientational polarization for side-chain polar polymers. In order to understand how much percentage of sulfone dipoles can rotate with a random orientation, we estimate the theoretical polarization, $P_{dip,theory}$, using the Langevin equation for freely rotating polar molecules[8,9,28]

$$P_{dip,theory} = N\mu_{RU}\left(\coth u - \frac{1}{u}\right), \text{ here } u = \frac{\mu_{RU}E}{k_BT} \quad (1)$$

where N is the repeat unit density ($N = 4.36 \times 10^{27}/\text{m}^3$ for PMSEMA), μ_{RU} the dipole moment of the repeat unit (μ_{RU} is 4.25 D for the sulfone group only and 6.0 D for combined sulfone and ester groups), E the applied electric field, k_B the Boltzmann constant, and T the absolute temperature. At $E = 100$ MV/m, theoretical $P_{dip,theory}$ values for PMSEMA at −50

Figure 6. Bipolar D-E loops for (A) a solution-cast PMSEMA film (26.1 μm) and (B) a commercial PMMA film (49 μm) at 25 °C. (C) Stored and discharged energy densities and (D) loss % for PMSEMA and PMMA at room temperature. The poling frequency is 20 Hz.

and 50 °C are calculated to be 9.48 and 18.0 mC/m^2, respectively. Here, we consider that only sulfone groups polarize at −50 °C (μ_{RU} = 4.25 D) and both sulfone and ester groups polarize at 50 °C (μ_{RU} = 6.0 D). Experimental polarization ($P_{dip,exp}$) due to dipolar motion for PMSEMA can be estimated as[28]

$$P_{dip,exp} = P_T - P_{-150\,°C}(1\ MHz)$$
$$= [\varepsilon_{r,T} - \varepsilon_{r,-150\,°C}(1\ MHz)]\varepsilon_0 E \qquad (2)$$

where P_T and $P_{-150\,°C}$(1 MHz) are polarizations, and $\varepsilon_{r,T}$ and $\varepsilon_{r,-150\,°C}$(1 MHz) are relative permittivity from BDS results at T and −150 °C, respectively. At −150 °C and high frequency (e.g., 1 MHz), we consider that the dielectric contribution to permittivity only originates from electronic and vibrational polarizations, and $\varepsilon_{r,-150\,°C}$(1 MHz) = 5.0. Assuming the electronic and vibrational polarizations are nearly independent of temperature,[9,40] the $P_{dip,exp}$ values at 100 MV/m for PMSEMA at −50 and 50 °C (1 Hz) are calculated to be 3.72 and 6.64 mC/m^2, respectively. Considering that the ratio of $P_{dip,exp}/P_{dip,theory}$ may represent the percentage of dipole flipping, the ratios are 39% and 37% at −50 and 50 °C, respectively. The similar $P_{dip,exp}/P_{dip,theory}$ ratios at −50 and 50 °C further confirm our earlier conclusion that the strong γ transition is only due to the polarization of sulfone groups and the weak β transition originates from the combined polarization of sulfone and ester groups. Both ratios are significantly higher than that (10%) reported for the CN-PC,[29] suggesting that sulfone and/or ester groups are more advantageous than the −CH$_2$CN groups in enhancing the dielectric constant of polymers.

The above studies focus on dielectric properties at low electric fields. In real dielectric applications, high electric fields are usually applied. High electric field dielectric properties were first studied by D-E hysteresis loop measurements for the hot-pressed PMSEMA film (42.5 μm thick). Centered bipolar D-E loops are shown in Figure 5. At 25 °C, narrow linear D-E loops were observed up to 182 MV/m from 20 to 2000 Hz. From the slope of these linear D-E loops, the apparent k could be determined as $k = D/(\varepsilon_0 E)$. Alternatively, the dynamic relative permittivity k' can also be defined as $k' = \partial D/(\varepsilon_0 \partial E)$. As we can see from Figure S2 in the Supporting Information, $k \approx k'$ within the ±200 MV/m range. This suggests that the nonlinearity for PMSEMA at 20 Hz and 25 °C can be negligible. It was observed that k values slightly increased with increasing the poling field or decreasing the poling frequency. For example, at 182 MV/m, k = 11.8 at 2000 Hz and 12.4 at 20 Hz. These k values were generally consistent with those in the above BDS results. When the temperature was increased to 50 °C (Figure 5D−F) and 75 °C (Figure 5G−I), relatively narrow and linear D-E loops were still observed, with slightly decreased maximum poling field and increased loop hysteresis, especially for 20 Hz. This could be attributed to enhanced dipole switching and certain impurity ion migration as the temperature approached the glass transition. Note that fresh samples were used for each poling frequency until a maximum poling field was reached. It was the different quality in each fresh hot-pressed sample that caused different maximum poling fields in Figure 5. These maximum poling fields cannot be simply considered as the Weibull breakdown strength. We also note that the hysteresis loss for PMSEMA at 75 °C is much lower than those for e-beamed P(VDF-TrFE) and P(VDF-TrFE-CFE) at the same temperature (see Figure S5 in the Supporting Information of

ref 38). This could be attributed to high ionic and electronic conductions in the high temperature paraelectric phases for P(VDF-TrFE)-based random copolymers. From these results, we concluded that the high dielectric constant and low loss dielectric properties persisted into high electric fields and they could again be attributed to the dipolar polarization of strong sulfone dipoles in PMSEMA.

In addition to the hot-pressed film, a solution-cast PMSEMA film (26.1 μm) was also obtained by drop-casting from redistilled DMF. Bipolar D-E loops of the solution-cast PMSEMA film and a commercial PMMA film (49 μm) at 25 °C and 20 Hz are shown in Figure 6. Due to a thinner film thickness and better film quality, the solution-cast PMSEMA film exhibited a higher maximum poling field, up to 283 MV/m, as compared to the hot-pressed PMSEMA film in Figure 5. Above 180 MV/m, the tips of the D-E loops slightly tilted up, possibly due to flipping of additional sulfonyl dipoles which were originally difficult to rotate in the sample. Note that the $P_{dip,exp}/P_{dip,theory}$ ratio was about 37%, indicating that not all dipoles had responded to the external electric field. This could be attributed to the random orientation of methylsulfonyl groups and/or not large enough free volume in the glassy PMSEMA. At a high enough electric field, these difficult-to-rotate dipoles started to rotate, resulting in a further increase in the total D value. For comparison, bipolar D-E loops for a commercial PMMA film are shown in Figure 6B. PMMA exhibited a lower k value of ca. 4.5 at room temperature, and the loops were somewhat broader than those for the solution-cast PMSEMA film. It was reported that the β transition of PMMA was located around 25 °C at 1 Hz.[33] Therefore, the broadening in its D-E loops could be attributed to the methyl ester dipole relaxation in PMMA around room temperature.

The stored ($U_{e,stored}$) and discharged ($U_{e,discharged}$) energy densities can be obtained from D-E loops and are compared for PMSEMA and PMMA in Figure 6C. Solution-cast and hot-pressed PMSEMA films exhibited similar discharge energy densities, although the charged energy density was slightly higher for the solution-cast PMSEMA film. Obviously, the discharge energy density for PMSEMA was much higher than that for PMMA at the same poling electric field. For example, at 200 MV/m, PMSEMA had a discharge energy density of 2.18 J/cm³, which was 3.2 times that of PMMA, while the loss %, defined as $100(1 - U_{e,discharged}/U_{e,stored})\%$,[41−43] for PMMA was much higher than those for the solution-cast and hot-pressed PMSEMA films (see Figure 6D). This again could be attributed to dipole switching during the β transition around room temperature for PMMA. Because the γ transition for PMSEMA was around −93 °C at 20 Hz, the losses for PMSEMA were lower than that for PMMA. Note that the loss for the solution-cast PMSEMA film was slightly higher than that for the hot-pressed PMSEMA film, which might be attributed to the different film preparation methods. For example, the solution-casting method might introduce additional residue solvent (DMF) and impurity ions in the sample, which could eventually increase the dielectric loss. Actually, we have run ¹H NMR for the PMSEMA sample, but could not detect any trace of DMF within the instrument limit, indicating that the content of residue solvent must be less than 0.1−0.5% (i.e., about the ¹H NMR limit). On the basis of our recent studies on PVDF and its copolymers,[38,39] even ppm levels of impurity ions can cause significant dielectric loss. It is probable that the residue content could be around the ppm level in solution-cast PMSEMA. Note that such a small amount of residue impurity

will not substantially decrease the breakdown strength of polymer films. For example, biaxially stretched PVDF films, which usually contain ppm levels of impurity ions inherited from suspension polymerization,[44] still shows a high DC breakdown strength greater than 700 MV/m.[45]

4. CONCLUSIONS

In summary, we have demonstrated a model dipolar glass polymer, PMSEMA, which exhibited a high permittivity (11.4 at 1 Hz and 10.5 at 1 kHz) and relatively low loss (tan δ ~ 0.02) at room temperature. Due to strong dipolar interactions, the glass transition of PMSEMA was at 109 °C, much higher than the T_g (ca. 20 °C) of the analogue polymer, PnBMA. Due to the small size and large dipole moment (4.25 D) of the side-chain sulfone groups, a strong γ transition was observed at ca. −110 °C. This strong γ transition increased the dielectric constant of PMSEMA from ca. 5.0 at −150 °C (at 1 MHz) to 9.2 at −50 °C (at 1 Hz). Considering the nature of the β transition in polymethacrylates with alkyl side chains (i.e., the rotation of the ester side groups between 10 and 60 °C at 1 Hz[33,34]), a weak β transition was assigned between 0 and 60 °C for combined polarization of sulfone and ester dipoles in PMSEMA. Due to this β transition, the dielectric constant further increased to 12.5 at 50 °C at 1 Hz. From frequency-scan BDS, the relaxation of sulfone dipoles was as fast as ~1 μs at room temperature. The dipole switching percentage of the sulfone groups was estimated as high as 37−39% in PMSEMA, much higher than that in −CH₂CN containing polymers. D-E loop studies indicated that the high dielectric properties persisted to high electric fields. The discharged energy density was nearly 3 times that of PMMA, whereas the dielectric loss was only 1/3−1/2 of that of PMMA. These experimental results suggest that PMSEMA is a good candidate for high energy density and low loss polymer dielectric at room temperature.

However, there are still opportunities to further improve dielectric properties of a dipolar glass polymer, such as PMSEMA. First, uniaxial stretching should be able to further increase dipolar polarization and thus the dielectric constant of PMSEMA, because uniaxial alignment of polymer chains will facilitate dipole rotation in the side chains. A similar orientational effect on dielectric constant is seen for PVDF and PVDF-graft copolymers.[39,46] Second, the number of CH₂ groups between the sulfone and ester groups can be varied to find the optimal dielectric properties. We expect that one CH₂ group between sulfone and ester groups may further increase the T_g and enhance the coupling between the sulfone and ester groups. On the contrary, more than two CH₂ groups will decrease the T_g and thus decrease the temperature window between the γ and α transitions. Third, the dissipation factor of 0.02 is still considered high for practical electrical and power applications. From the lesson of the methyl ester group rotation in PMMA,[35] we speculate that the free volume might not be large enough to allow friction free rotation of sulfone dipoles. Therefore, it is desirable to slightly increase the free volume in dipolar glass polymers. Fourth, to obtain high T_g values (e.g., above 150 °C), the main-chain rigidity must be increased in order to avoid a potential decrease in T_g due to the increase in free volume of the glassy polymer. This requires utilization of rigid-rod backbone polymers such as polyimides.[30] Research is currently underway to develop better dipolar glass polymers to achieve high energy density and high temperature capability while maintaining low dielectric losses.

ASSOCIATED CONTENT

$\textbf{S}$ Supporting Information

Verification of sample preparation for dielectric property studies and apparent dielectric constant versus dynamic dielecteric constant for PMSEMA. This material is available free of charge via the Internet at http://pubs.acs.org.

AUTHOR INFORMATION

Corresponding Authors

*E-mail: mhl2@case.edu (M.H.L).
*E-mail: lxz121@case.edu (L.Z.).

Notes

The authors declare no competing financial interest.

ACKNOWLEDGMENTS

REFERENCES

(1) Zhu, L. Exploring Strategies for High Dielectric Constant and Low Loss Polymer Dielectrics. *J. Phys. Chem. Lett.* **2014**, *5*, 3677−3687.

(2) Zhu, L.; Wang, Q. Novel Ferroelectric Polymers for High Energy Density and Low Loss Dielectrics. *Macromolecules* **2012**, *45*, 2937−2954.

(3) Chu, B.; Zhou, X.; Ren, K.; Neese, B.; Lin, M. R.; Wang, Q.; Bauer, F.; Zhang, Q. M. A Dielectric Polymer with High Electric Energy Density and Fast Discharge Speed. *Science* **2006**, *313*, 334−336.

(4) Liu, P.; Yen, R.; Bloembergen, N. Dielectric-Breakdown Threshold, 2-Photon Absorption, and Other Optical Damage Mechanisms in Diamond. *IEEE J. Quantum Electron.* **1978**, *14*, 574−576.

(5) Ho, J.; Ramprasad, R.; Boggs, S. Effect of Alteration of Antioxidant by UV Treatment on the Dielectric Strength of BOPP Capacitor Film. *IEEE Trans. Dielectr. Electr. Insul.* **2007**, *14*, 1295−1301.

(6) Sun, Y.; Bealing, C.; Boggs, S.; Ramprasad, R. 50+ Years of Intrinsic Breakdown. *IEEE Electr. Insul. Mag.* **2013**, *29*, 8−15.

(7) Ceresoli, D.; Righi, M. C.; Tosatti, E.; Scandolo, S.; Santoro, G.; Serra, S. Exciton Self-Trapping in Bulk Polyethylene. *J. Phys.: Condens. Matter* **2005**, *17*, 4621−4627.

(8) Kao, K.-C. *Dielectric Phenomena in Solids: With Emphasis on Physical Concepts of Electronic Processes*; Elsevier Academic Press: Boston, 2004.

(9) Blythe, A. R.; Bloor, D. *Electrical Properties of Polymers*, 2nd ed.; Cambridge University Press: Cambridge, 2005.

(10) Wang, C. C.; Pilania, G.; Boggs, S. A.; Kumar, S.; Breneman, C.; Ramprasad, R. Computational Strategies for Polymer Dielectrics Design. *Polymer* **2014**, *55*, 979−988.

(11) Kremer, F.; Schönhals, A. *Broadband Dielectric Spectroscopy*; Springer: Berlin, 2003.

(12) Kim, S. H.; Hong, K.; Xie, W.; Lee, K. H.; Zhang, S. P.; Lodge, T. P.; Frisbie, C. D. Electrolyte-Gated Transistors for Organic and Printed Electronics. *Adv. Mater.* **2013**, *25*, 1822−1846.

(13) Nalwa, H. S. *Ferroelectric Polymers: Chemistry, Physics, and Applications*; Marcel Dekker: New York, 1995.

(14) Yang, L.; Li, X.; Allahyarov, E.; Taylor, P. L.; Zhang, Q. M.; Zhu, L. Novel Polymer Ferroelectric Behavior via Crystal Isomorphism and the Nanoconfinement Effect. *Polymer* **2013**, *54*, 1709−1728.

(15) Zhang, Q. M.; Bharti, V.; Zhao, X. Giant Electrostriction and Relaxor Ferroelectric Behavior in Electron-Irradiated Poly(vinylidene fluoride-trifluoroethylene) Copolymer. *Science* **1998**, *280*, 2101−2104.

(16) Bharti, V.; Zhao, X. Z.; Zhang, Q. M.; Romotowski, T.; Tito, F.; Ting, R. Ultrahigh Field Induced Strain and Polarization Response in Electron Irradiated Poly(vinylidene fluoride-trifluoroethylene) Copolymer. *Mater. Res. Innovations* **1998**, *2*, 57−63.

(17) Chung, T. C.; Petchsuk, A. Synthesis and Properties of Ferroelectric Fluoroterpolymers with Curie Transition at Ambient Temperature. *Macromolecules* **2002**, *35*, 7678−7684.

(18) Xia, F.; Cheng, Z.; Xu, H.; Li, H.; Zhang, Q.; Kavarnos, G. J.; Ting, R. Y.; Abdul-Sedat, G.; Belfield, K. D. High Electromechanical Responses in a Poly(vinylidene fluoride-trifluoroethylene-chlorofluoroethylene) Terpolymer. *Adv. Mater.* **2002**, *14*, 1574−1577.

(19) Lu, Y.; Claude, J.; Neese, B.; Zhang, Q.; Wang, Q. A Modular Approach to Ferroelectric Polymers with Chemically Tunable Curie Temperatures and Dielectric Constants. *J. Am. Chem. Soc.* **2006**, *128*, 8120−8121.

(20) Lu, Y.; Claude, J.; Zhang, Q.; Wang, Q. Microstructures and Dielectric Properties of the Ferroelectric Fluoropolymers Synthesized via Reductive Dechlorination of Poly(vinylidene fluoride-co-chlorotrifluoroethylene)s. *Macromolecules* **2006**, *39*, 6962−6968.

(21) Dalton, L. Nonlinear Optical Polymeric Materials: From Chromophore Design to Commercial Applications. *Adv. Polym. Sci.* **2002**, *158*, 1−86.

(22) Wurthner, F.; Wortmann, R.; Meerholz, K. Chromophore Design for Photorefractive Organic Materials. *ChemPhysChem* **2002**, *3*, 17−31.

(23) Hains, P. J.; Williams, G. Molecular Motion in Polystyrene - Plasticizer Systems as Studied by Dielectric Relaxation. *Polymer* **1975**, *16*, 725−729.

(24) van den Berg, O.; Wubbenhorst, M.; Picken, S. J.; Jager, W. F. Characteristic Size of Molecular Dynamics in Polymers Probed by Dielectric Probes of Variable Length. *J. Non-Cryst. Solids* **2005**, *351*, 2694−2702.

(25) Priestley, R. D.; Broadbelt, L. J.; Torkelson, J. M.; Fukao, K. Glass Transition and α-Relaxation Dynamics of Thin Films of Labeled Polystyrene. *Phys. Rev. E* **2007**, *75*, 061806.

(26) Bendler, J. T.; Edmondson, C. A.; Wintersgill, M. C.; Boyles, D. A.; Filipova, T. S.; Fontanella, J. J. Electrical Properties of a Novel Fluorinated Polycarbonate. *Eur. Polym. J.* **2012**, *48*, 830−840.

(27) Wang, D. H.; Kurish, B. A.; Treufeld, I.; Zhu, L.; Tan, L.-S. Synthesis and Characterization of High Nitrile Content Polyimides as Dielectric Films for Electrical Energy Storage. *J. Polym. Sci., Part A: Polym. Chem.* **2014**, *53*, 422−436.

(28) Treufeld, I.; Wang, D. H.; Kurish, B. A.; Tan, L.-S.; Zhu, L. Enhancing Electrical Energy Storage Using Polar Polyimides with Nitrile Groups Directly Attached to the Main Chain. *J. Mater. Chem. A* **2014**, *2*, 20683−20696.

(29) Bendler, J. T.; Boyles, D. A.; Edmondson, C. A.; Filipova, T.; Fontanella, J. J.; Westgate, M. A.; Wintersgill, M. C. Dielectric Properties of Bisphenol A Polycarbonate and Its Tethered Nitrile Analogue. *Macromolecules* **2013**, *46*, 4024−4033.

(30) Bedekar, B. A.; Tsujii, Y.; Ide, N.; Kita, Y.; Fukuda, T.; Miyamoto, T. Dielectric Relaxation of Cyanoethylated Poly(2,3-dihydroxypropyl methacrylate). *Polymer* **1995**, *36*, 4735−4740.

(31) Mark, J. E. *Polymer Data Handbook*, 2nd ed.; Oxford University Press: Oxford, 2009.

(32) Pham, Q. T.; Pieraud, R.; Waton, H.; Llauro-Darricades, M.-F. *Proton and Carbon NMR Spectra of Polymers*, 5th ed.; Wiley: Chichester, 2003.

(33) Fried, J. R. Sub-*Tg* Transitions. In *Physical Properties of Polymers Handbook*; Mark, J. E., Ed.; Springer: New York, 2007; pp 217−232.

(34) Cowie, J. M. G.; Ferguson, R. Possible Origins of the *β*-Relaxation in Poly(methyl methacrylate) and Related Structures from Molecular Mechanics Calculations. *Polymer* **1987**, *28*, 503−508.

(35) Schmidt-Rohr, K.; Kulik, A. S.; Beckham, H. W.; Ohlemacher, A.; Pawelzik, U.; Boeffel, C.; Spiess, H. W. Molecular Nature of the *β*

Relaxation in Poly(methyl methacrylate) Investigated by Multidimensional NMR. *Macromolecules* **1994**, *27*, 4733−4745.

(36) Hoff, E. A. W.; Robinson, D. W.; Willbourn, A. H. Relation between the Structure of Polymers and Their Dynamic Mechanical and Electrical Properties. Part II. Glassy State Mechanical Dispersions in Acrylic Polymers. *J. Polym. Sci.* **1955**, *18*, 161−176.

(37) Mackey, M.; Schuele, D. E.; Zhu, L.; Flandin, L.; Wolak, M. A.; Shirk, J. S.; Hiltner, A.; Baer, E. Reduction of Dielectric Hysteresis in Multilayered Films via Nanoconfinement. *Macromolecules* **2012**, *45*, 1954−1962.

(38) Mackey, M.; Schuele, D. E.; Zhu, L.; Baer, E. Layer Confinement Effect on Charge Migration in Polycarbonate/Poly-(vinylidene fluoride-*co*-hexafluoropropylene) Multilayered Films. *J. Appl. Phys.* **2012**, *111*, 113702.

(39) Yang, L.; Allahyarov, E.; Guan, F.; Zhu, L. Crystal Orientation and Temperature Effects on Double Hysteresis Loop Behavior in a Poly(vinylidene fluoride-*co*-trifluoroethylene-*co*-chlorotrifluoroethylene)-*graft*-Polystyrene Graft Copolymer. *Macromolecules* **2013**, *46*, 9698−9711.

(40) Buldakov, M. A.; Matrosov, I. I.; Cherepanov, V. N. Temperature Dependence of Polarizability of Diatomic Homonuclear Molecules. *Opt. Spectrosc.* **2000**, *89*, 37−41.

(41) Guan, F.; Wang, J.; Pan, J.; Wang, Q.; Zhu, L. Effects of Polymorphism and Crystallite Size on Dipole Reorientation in Poly(vinylidene fluoride) and Its Random Copolymers. *Macromolecules* **2010**, *43*, 6739−6748.

(42) Guan, F.; Wang, J.; Yang, L.; Tseng, J. K.; Han, K.; Wang, Q.; Zhu, L. Confinement-Induced High-Field Antiferroelectric-like Behavior in a Poly(vinylidene fluoride-*co*-trifluoroethylene-*co*-chlorotrifluoroethylene)-*graft*-polystyrene Graft Copolymer. *Macromolecules* **2011**, *44*, 2190−2199.

(43) Guan, F.; Wang, J.; Yang, L.; Guan, B.; Han, K.; Wang, Q.; Zhu, L. Confined Ferroelectric Properties in Poly(Vinylidene Fluoride-*co*-Chlorotrifluoroethylene)-*graft*-Polystyrene Graft Copolymers for Electric Energy Storage Applications. *Adv. Funct. Mater.* **2011**, *21*, 3176−3188.

(44) Ameduri, B. From Vinylidene Fluoride (VDF) to the Applications of VDF-Containing Polymers and Copolymers: Recent Developments and Future Trends. *Chem. Rev.* **2009**, *109*, 6632−6686.

(45) Jow, T. R.; Cygan, P. J. Dielectric Breakdown of Polyvinylidene Fluoride and Its Comparisons with Other Polymers. *J. Appl. Phys.* **1993**, *73*, 5147−5151.

(46) Guan, F.; Pan, J.; Wang, J.; Wang, Q.; Zhu, L. Crystal Orientation Effect on Electric Energy Storage in Poly(vinylidene fluoride-*co*-hexafluoropropylene) Copolymers. *Macromolecules* **2010**, *43*, 384−392.